



14th IEA Heat Pump Conference
15-18 May 2023, Chicago, Illinois

Comparison of seasonal energy efficiency of different compressor types

Christian Stahel^a, Lukas Wick^a, Frank Tillenkamp^{a,*},
Silvan Steiger^a, Manuel Diem^a

^aZurich University of Applied Sciences, Institute of Energy Systems and Fluid Engineering,
Technikumstrasse 9, 8400 Winterthur, Switzerland

Abstract

In this work, the energetic behavior of compressor types was investigated and an evaluation method was developed to compare them under variable load profiles and locations. The numerous compressor maps, locations and load profiles lead to a very large number of possible combinations. For the efficient evaluation a freely available compressor tool has been developed which compares the different compressor types. The core of the tool is a database with compressor polynomials of more than 1400 compressors from different manufactures. The same compressor types from different manufacturers were grouped together to represent an average energy performance. Compressor characteristic maps were created which visualize the behavior of each compressor type as well as their application limits and control range. An evaluation method is used to determine the seasonal energy efficiency of the different compressor types depending on the location, load profile and application. The method is based on several operating points, which are weighted according to their energetic share of the annual consumption. Based on the maps, the seasonal efficiency of the compressor types is determined and ranked.

© HPC2023.

Selection and/or peer-review under the responsibility of the organizers of the 14th IEA Heat Pump Conference 2023.

Keywords: Compressor types, compressor characteristic map, seasonal efficiency

1. Introduction

The benefits of refrigeration technologies towards a sustainable energy system are undisputed. The market share of refrigeration machines and heat pump is increasing rapidly. The shortage of skilled workers is therefore becoming a major problem for the industry. On behalf of the Swiss Federal Office of Energy, we developed a freely available tool [4] to support planners in the selection of the optimal compressor type. The focus of this investigation is on air-conditioning and commercial refrigeration applications.

The aim of this work is an energetic comparison of different compressor types based on the data provided by the manufacturers. The performance data of compressors are provided in the form of polynomials and are regulated in the EN 12900 [1] standard. The behavior of the compressors can be summarized in compressor maps. Compressor maps are often created for turbo compressors in the form of shell curves [5][6][7]. However, compressor maps in refrigeration technology are usually not available.

In this study, compressor maps for different compressors were created based on the performance data of the compressor polynomials.

The seasonal comparison of refrigeration machines is regulated in EN 14825 [2]. Here, the seasonal efficiency is determined based on several operating points, which are weighted according to their energetic share. The energy weighting is based on hourly frequencies of ambient temperatures and load profiles. In this study, the SEER evaluation method was adapted to compressors. This allows a seasonal assessment of

* Corresponding author. Tel.: +41 (0) 58 934 73 61.
E-mail address: frank.tillenkamp@zhaw.ch

compressor types based on data provided by the manufacturers. For this purpose, compressor maps are combined with load profiles and weather data.

2. Compressor characteristic maps

The representation of compressor performance data is defined in the EN 12900 [1] standard. Compressor polynomials can be used to determine cooling capacity \dot{Q}_0 , electrical power consumption P_{el} and refrigerant mass flow \dot{m} as a function of evaporating temperature T_0 and condensing temperature T_c . The compressor polynomials are only valid for a specific frequency, overheating and subcooling. Therefore, several polynomials are required for each compressor to represent the compressor map. Table 1 shows an overview of the collected polynomials.

Table 1. Overview compressor polynomial parameters

Refrigerant	overheating	subcooling	frequency
R1234ze / R454B / R513A / R449A / R744	10 K	0 K	$f_{\min} - f_{\max}$
R290	20 K	0 K	$f_{\min} - f_{\max}$
R717	5 K	0 K	$f_{\min} - f_{\max}$

The coefficients of the compressor polynomials are available in the design tools of the manufacturers. Manufacturers who do not provide their compressor data could not be considered in this study. For turbo compressors are no performance polynomials according to EN 12900 available, therefore only individual operating points are given. These were calculated using the manufacturers' design tools.

Additional quantities such as Coefficient of Performance COP , final compression temperature T_2 and isentropic compressor efficiency η_{is} can be calculated directly from the given compressor polynomials.

2.1. Database (compressor polynomials)

The application of the refrigeration machine has a strong impact on the evaporating temperature of the plant. Therefore, three different applications with different design points are considered in this study. Depending on the application, various refrigerants and design capacities were investigated. Table 2 shows an overview of the selections considered.

Table 2. Overview selections

Application	Design Point (T_0 / T_c)	Design capacity (\dot{Q}_{0_design})	Refrigeration
Air conditioning	5 / 45 °C	20 / 50 / 100 / 300 kW	R1234ze / R290 / R454B / R513A / R717 / R744
Medium temperature	-10 / 45 °C	2 / 10 / 50 / 100 kW	R449A / R513A / R744
Low temperature	-30 / 40 °C	1 / 5 / 25 / 50 kW	R449A / R744

Any combination of application, refrigeration capacity and refrigerant for each compressor type represents a selection. For each selection, compressor data from several manufacturers are collected according to the parameters shown in Table 1. In total, more than 1400 compressors were considered. Figure 1 shows the collected data for semi-hermetic propane reciprocating compressors with a design capacity \dot{Q}_{0_design} of 50 kW \pm 30% from various manufacturers.

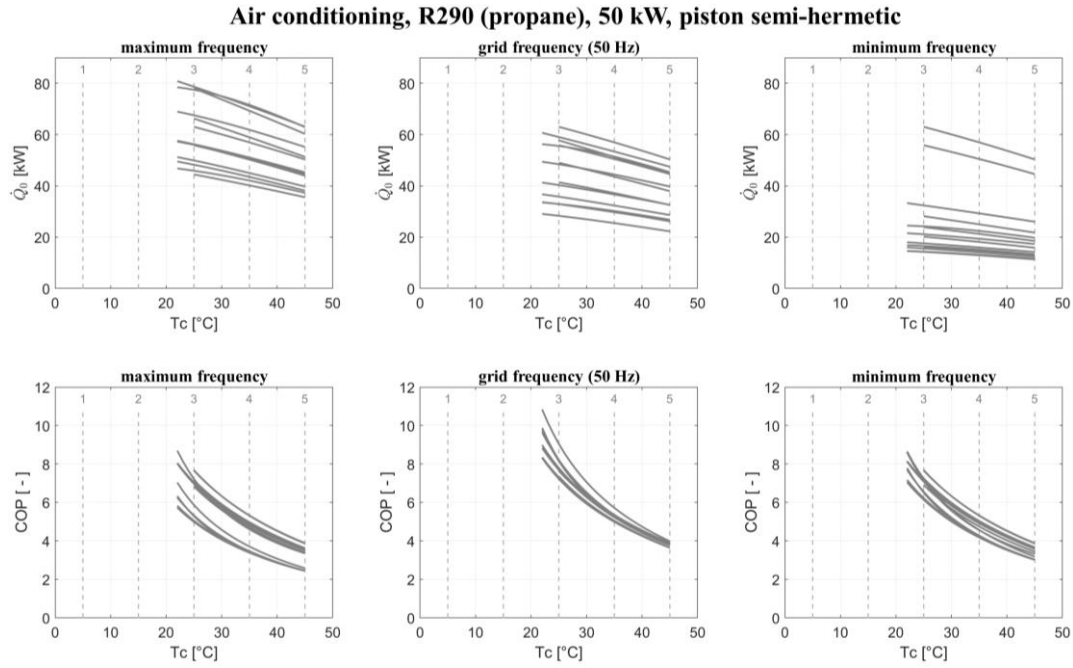


Fig. 1. Compressor data of a selection

In Figure 1 the cooling capacity \dot{Q}_0 and the Coefficient of Performance COP of each compressor as a function of the condensing temperature T_c at various frequencies are illustrated. The evaporating temperature T_0 is constant according to the design point. The deviations of \dot{Q}_0 at the maximum frequency with $T_c = 45$ °C are due to the capacity range considered ($\dot{Q}_{0_design} \pm 30\%$). It should be noted that the frequency range may differ depending on the manufacturer. Additionally, the operating limit $T_{c,min}$ of each compressor is taken into account.

2.2. Neutralization

The aim of this study is to compare different types of compressors. To prevent direct comparison between manufacturers, neutralization is applied. In the following, it will be shown how this neutralization is implemented. The compressor data from different manufacturers are combined into one average compressor with each manufacturer equally weighted. This resulting compressor represents the average behavior of the compressor type in the specific selection. Figure 2 shows the compressor characteristic map for the neutralized compressor. This compressor map is based on the twelve individual compressors shown in figure 1.

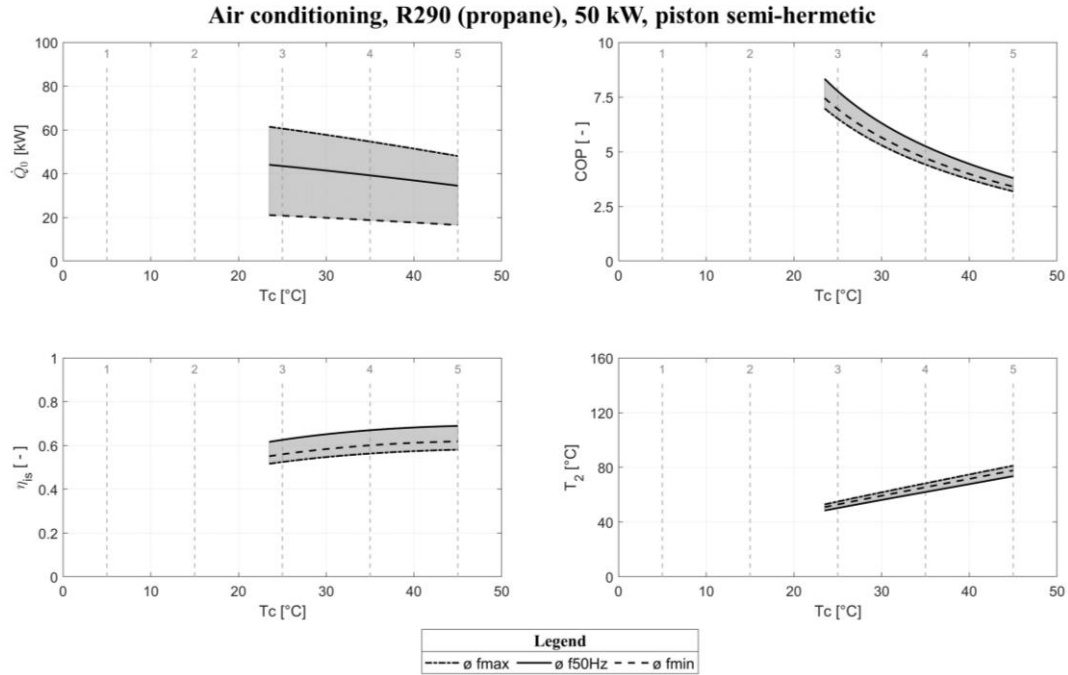


Fig. 2. Compressor characteristic map of a semi-hermetic propane reciprocating compressor

In Figure 2 the compressor characteristic map of a semi-hermetic propane reciprocating compressor with a $\dot{Q}_{0, \text{design}}$ of 50 kW for air conditioning applications ($T_0 = 5^\circ\text{C}$) is shown. The curve of the cooling capacity \dot{Q}_0 at different frequencies shows the control range at variable condensing temperatures T_c . The left end of the characteristic diagram corresponds to the average operating limit. The right diagram shows the course of the COP at different frequencies.

The compressor maps are the basis for seasonal efficiency considerations. However, they also allow an assessment of conceptual considerations when planning a plant. For example, the effects of oversized refrigeration systems or compressors can be easily estimated from the compressor map.

2.3. Comparison of different compressor maps

A total of 70 compressor maps were created during the investigation. These maps are located in the appendix of the final project report [3]. To show the differences between the compressor types, sizes or refrigerants used, the compressor maps were also compared. This comparison illustrates the deviations in efficiency, operating limits, and control range. Therefore, this comparison is a very comprehensive resource. Figure 3 is pointing out the deviation of different compressor types with a 2 kW design capacity and the refrigerant R513A. Further comparisons for other selections can be seen in the final report [3].

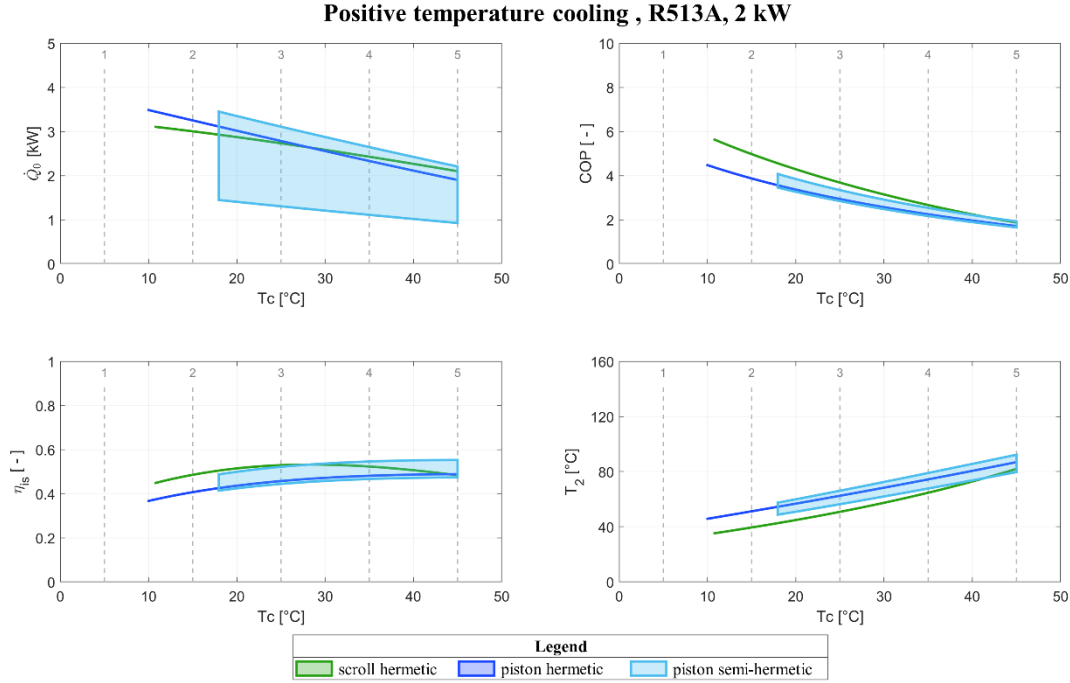


Fig. 3. Comparison compressor characteristic map of different compressor types

The selection in Figure 3 compares compressor types in medium temperature application ($T_0 = -10\text{ °C}$). Due to the small design capacity \dot{Q}_{0_design} selected, no turbo or screw compressors are available. The hermetic piston and scroll compressors don't have capacity control, the compressor map therefore merges into one curve.

At the design point ($T_c = 45\text{ °C}$), the cooling capacity \dot{Q}_0 of the reciprocating compressor and the scroll compressor is almost identical. If the condensing temperature T_c is reduced, the cooling capacity \dot{Q}_0 of the reciprocating compressor increases significantly more than the one of the scroll compressor. As a result of re-expansion, the volumetric efficiency of the reciprocating compressor increases more in comparison to the scroll compressor if a small pressure differential is applied. Therefore, mass flow of the reciprocating compressor and thus capacity \dot{Q}_0 increase over-proportionally at low condensing temperatures T_c .

The internal pressure ratio is particularly characteristic for the behavior of the scroll compressor. This can be seen in the curve of the isentropic compressor efficiency η_{is} . If the pressure ratio of the system and the internal pressure ratio of the compressor match, high efficiencies are achieved. If the compressor is operated at a different pressure ratio, the efficiency is increasingly reduced. When selecting a scroll compressor, it is therefore important to ensure that the internal pressure ratio is at an energetically relevant operating point.

3. Seasonal energy efficiency evaluation method (aCOP)

The seasonal energy efficiency ratio SEER is a seasonal assessment of chillers and is defined in EN 14825. However, due to the different system boundaries as shown in figure 4, the ratio cannot be used to evaluate compressors. For the evaluation of compressor types, the ratio aCOP (annual coefficient of performance) is defined. The methodology of the aCOP is very much based on the existing ratio (SEER) of chillers in part-load operation and is an energetic analysis. The aCOP is calculated according to Eq 1.

$$aCOP = \sum_{i=1}^5 w_i \cdot c_i \cdot COP_i \quad (1)$$

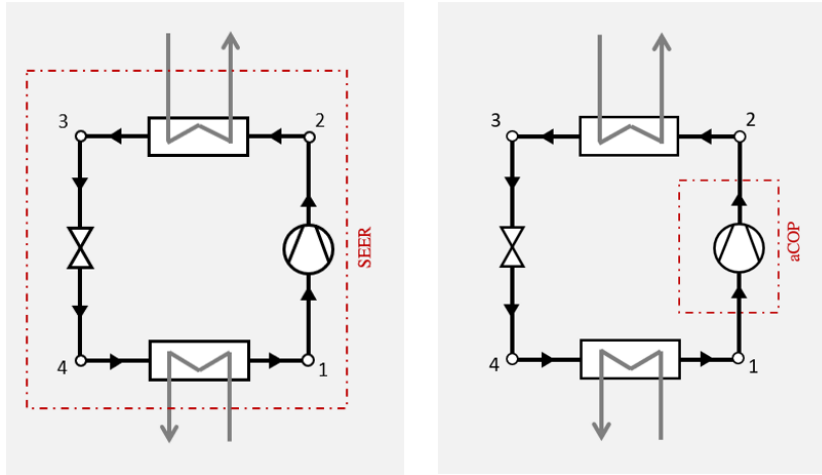


Fig. 4. System boundary SEER and aCOP

To compare different chillers, EN 14825 tests chillers under identical inlet and outlet temperatures in the evaporator and condenser. The temperatures and load profiles are defined to determine a seasonal behavior. The aCOP applies the same methodology to the system boundary compressor. Different compressors are compared under the same evaporating and condensing temperatures.

To calculate the annual coefficient of performance aCOP the compressor maps are combined with load profiles and hourly frequencies of ambient temperatures. This ratio is based on five operating points. The COP of the compressor COP_i is determined from the compressor map. The energetic share of the annual consumption w_i is calculated from the load profile and the hourly frequency of the ambient temperatures. If the cooling capacity of the compressor cannot be adapted to the cooling demand due to the limitations of the capacity control, the COP at the operating point is reduced with a type-dependent cycle factor c_i . In this study, several load profiles and Swiss locations were investigated. The impact of location and load profile are shown in Figure 5.

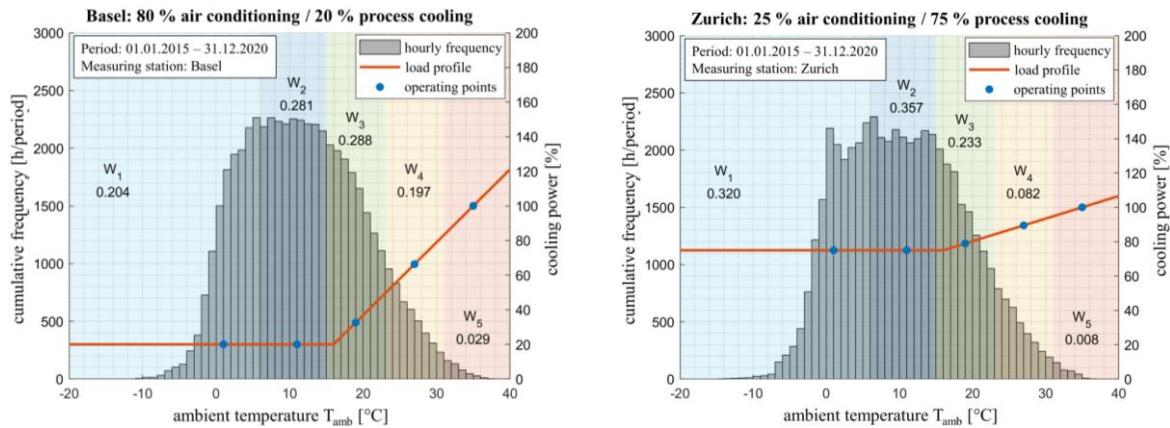


Fig. 5. Influence of location and load profile on weighting

Figure 6 shows the influence of load profile and location on the weighting of the individual operating points. The location has an impact on the frequency of ambient temperatures T_{amb} . This can be seen from the heights of the bars. The load profile shows the cooling capacity \dot{Q}_0 in relation to the ambient temperature T_{amb} . The weather data are taken from the data portal IDAweb of the Federal Office of Meteorology and Climatology MeteoSwiss. The hourly average temperature of the years 2015-2020 is used.

3.1. Compressor performance

To determine the coefficient of performance COP of the compressor from the compressor map, the cooling demand \dot{Q}_{dem} , evaporating temperature T_0 and condensing temperature T_c has to be defined. The cooling

demand and evaporating temperature are given due to the load profile and application. The condensing temperature depends on the ambient temperature T_{amb} and the operating limit T_{c_min} of the compressor. Thus, the operating point of the compressor may vary depending on the compressor type. Table 3 shows the correlation between the ambient temperature T_{amb} and the condensing temperature T_c regarding the operating limit T_{c_min} of the compressor.

Table 3. Operating Points

Operating point	T_{amb} [°C]	ΔT [°C]	$T_{c_theoretical}$ [°C]	T_{c_min} [°C]	T_c [°C]
1	1	4	5	10	10
2	11	4	15	10	15
3	19	6	25	10	25
4	27	8	35	10	35
5	35	10	45	10	45

The temperature difference ΔT between ambient temperature T_{amb} and theoretical condensing temperature $T_{c_theoretical}$ is not constant for all operating points. This is because the temperature differences dT in the heat exchangers become smaller in part-load operation. The defined temperature differences correspond to an application with dry cooler. If the theoretical condensing temperature $T_{c_theoretical}$ is smaller than the compressor operating limit T_{c_min} , the condensing temperature T_c will be adjusted. The impact of the compressor map on the operating point is shown in Fig. 6.

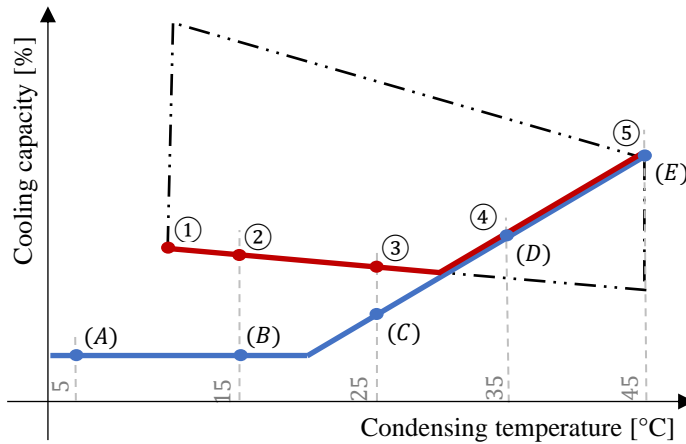


Fig. 6. Influence of compressor map on operating points

Figure 6 shows the differences between theoretical conditions and operating conditions. The theoretical conditions (A-E) resulting from the ambient temperatures T_{amb} and the cooling demand \dot{Q}_{dem} based on the load profile (blue). The operating conditions (① - ⑤) are resulting from the combination of compressor map and theoretical conditions. The operating conditions (red) are therefore depending on the operating limits and control range of the compressor. Thus, the operating points of the compressor types may differ at the same ambient temperatures.

3.2. Operating mode

The cycling factor c_i is determined from the combination of load profile and compressor map. If the cooling demand \dot{Q}_{dem} is within the compressor map, the compressor can modulate and adapt the compressor capacity \dot{Q}_{comp} to the cooling demand. If the cooling demand is less than the cooling capacity at minimum frequency, the compressor goes into on-off operation. This short cycling has a negative influence on the efficiency. The operating mode thus has an influence on the efficiency of the compressor and is considered by a cycling factor c_i . The cycling factor c_i depends on the compressor type and the difference between the

cooling demand \dot{Q}_{dem} of the consumer and the cooling capacity of the compressor \dot{Q}_{comp} and is calculated according to the equations 2 and 3.

$$c_i = \frac{f_{load}}{f_v * f_{load} + (1 - f_v)} \quad (2)$$

$$f_{load} = \frac{\dot{Q}_{dem}}{\dot{Q}_{comp}} \quad (3)$$

The calculation of the cycling factor c_i is very similar to EN 14825. First, according to equation 3, the load factor f_{load} is calculated from the cooling demand \dot{Q}_{dem} and the capacity of the compressor \dot{Q}_{comp} . The load factor f_{load} can take values between 0 and 1 and becomes smaller the more the compressor is short cycling. Subsequently, the cycling factor c_i can be calculated according to equation 2. For this, the load factor f_{load} and the reduction factor f_v of the compressor type are required. The reduction factor can be determined using Table 4.

Table 4. Reduction factor compressor types

Compressor Type	f_v
Rolling piston	0.9
Scroll	0.9
Reciprocating	0.9
Screw	0.85
Turbo	0.8

As shown in Table 4, the reduction factor f_v depends on the compressor type. This is since the influence of the on-off operation on the efficiency varies depending on the compressor type. A turbo compressor has very high speeds and therefore requires energetically demanding switch-on and switch-off routines. For this reason, the differences in compressor types are addressed in the reduction factor f_v . It should be mentioned that the values of the factors were defined in consultation with experts. In further investigations, the values can be validated and optimized.

3.3. Energetic weighting

The concept of energy weighting is already shown in Figure 4. Each operating point covers a range of ambient temperatures T_{amb} . The weighting of the operating point is the ratio of the cooling load in the temperature range to the annual cooling load and is calculated according to equation 3.

$$w_x = \frac{\sum_{x_{min}}^{x_{max}} (h_i * \dot{Q}_{demand_i})}{\sum_{-20}^{40} (h_i * \dot{Q}_{demand_i})} \quad (4)$$

The weighting factors are depending on the load profile as well as the location. The location defines how many hours a year a certain ambient temperature h_i occurs. The load profile determines the cooling demand \dot{Q}_{dem} at a certain ambient temperature. The cooling load corresponds to the product of cooling demand and frequency at a specific ambient temperature. The sum of all weighting factors is always 1. The temperature ranges of the operating points are shown in table 5.

Table 5. Temperature range weighting factors

Weighting factor	Temperature Range	
	Min.	Max.
w_1	-20 °C	6 °C
w_2	6 °C	15 °C
w_3	15 °C	23 °C
w_4	23 °C	31 °C
w_5	31 °C	40 °C

4. Results

4.1. Compressor characteristic maps

In this study, manufacturer-neutral compressor maps were created for different compressor types, refrigerants, and sizes. The characteristic compressor maps can be used regardless of the presented evaluation method (aCOP) and show their seasonal behavior. Based on the information presented, such as the operating limits, control range or efficiencies, many conceptual impacts can be estimated. In particular, the comparison of compressor maps as shown in Figure 7 clarify the differences between compressor types.

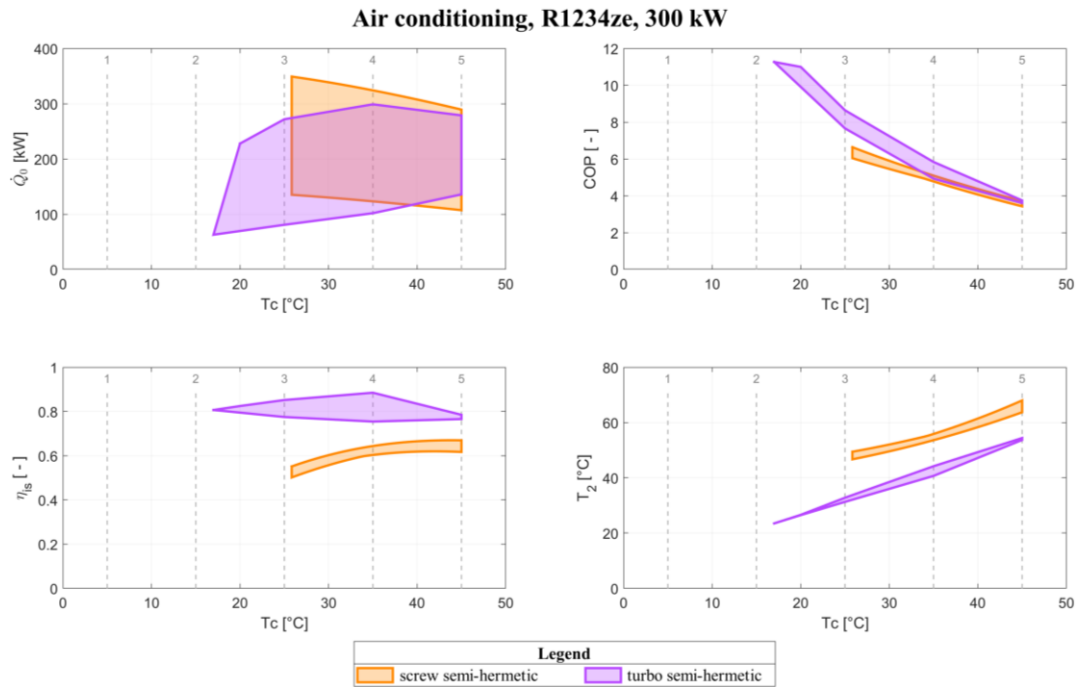


Fig. 7. Comparison of compression principles

Figure 7 shows the deviation between a displacement compressor (screw) and a fluid machine (turbo). In particular, the trend of the cooling capacity \dot{Q}_0 as a function of the condensing temperature T_c is most interesting. Cooling demand decreased in many applications as ambient temperatures dropped. Turbo compressors can modulate the cooling capacity \dot{Q}_0 to a much greater extent as the condensing temperature T_c drops. It should be noted that the compressor data of the turbo compressors do not consist of polynomials according to EN 12900.

4.2. Seasonal energy efficiency evaluation method (aCOP)

The presented evaluation methodology combines compressor maps with load profiles and weather data from locations and allows an energetic comparison of compressor types. Due to the large number of applications,

refrigerants, cooling capacities, load profiles and locations investigated, a very large number of results have been obtained.

For the efficient evaluation of a specific plant, a compressor tool has been developed which compares compressor types on the basis of a few parameters and supports the selection of the optimum compressor type by providing further additional information. The tool can be downloaded free of charge from the Federal Office for Energy [4]. Figure 8 shows an example of the evaluation of a selection.

Ranking	Compressor-Type	Annual Coefficient of Performance	t _{amb}	t _c	COP Average	COP Low - Best	Load Profile
1	Reciprocating semi hermetic	aCOP (Average) 6.4	1 °C	19 °C	8.3	(5.9 - 10.0)	4 kW
			11 °C	19 °C	8.3	(5.9 - 10.0)	4 kW
		aCOP (Low - Best) (4.7 - 7.6)	19 °C	25 °C	6.4	(4.8 - 7.6)	6.5 kW
			27 °C	35 °C	4.7	(3.9 - 5.1)	13 kW
			35 °C	45 °C	3.1	(1.9 - 3.4)	20 kW
2	Scroll hermetic	aCOP (Average) 5	1 °C	21 °C	7.5	(6.8 - 8.5)	4 kW
			11 °C	21 °C	7.5	(6.8 - 8.5)	4 kW
		aCOP (Low - Best) (4.4 - 5.6)	19 °C	25 °C	6.6	(6.1 - 7.1)	6.5 kW
			27 °C	35 °C	5	(4.7 - 5.3)	13 kW
			35 °C	45 °C	3.7	(3.4 - 3.9)	20 kW
3	Reciprocating hermetic	aCOP (Average) 4.1	1 °C	16 °C	7.1	(6.3 - 7.9)	4 kW
			11 °C	16 °C	7.1	(6.3 - 7.9)	4 kW
		aCOP (Low - Best) (3.7 - 4.5)	19 °C	25 °C	5.6	(5.2 - 5.9)	6.5 kW
			27 °C	35 °C	4.3	(4.1 - 4.4)	13 kW
			35 °C	45 °C	3.2	(3.1 - 3.3)	20 kW

Fig. 8. Example results compressor tool

Figure 8 shows the ranking of R513A compressors with a cooling capacity of 20 kW in an air conditioning application. Only scroll and reciprocating compressors are available in this capacity range. The ranking is made according to the average aCOP. This is calculated according to equation 1. The aCOP average is determined from all compressors in the selection. In addition, the aCOP of the best and worst compressor of the selection (low – best) as well as details of the individual operating points are shown. The results of the tool were randomly checked by the experts who accompanied the project.

5. Conclusion

The created compressor maps are a tool to estimate conceptual considerations. The representation of the seasonal behavior in combination with the control range and the operating limit allow a very comprehensive comparison. This is especially helpful for prospective professionals to better understand the differences in compressor types.

Some of the compressor manufacturers were in the process of converting their product line to the refrigerants studied. Therefore, it is possible that certain compressor data were not yet available at the time of data collection and are therefore not shown. The data basis for the creation of the compressor maps should therefore be updated later. In addition, further distinctions (e.g. three-phase asynchronous motors or permanent magnet motors) could be made to further subdivide the maps in order to better represent differences between series.

The polynomials provided by the manufacturers allow very extensive comparisons regarding the seasonal efficiency of compressors. The evaluation method developed in this thesis adapts the methodology of the SEER to a compressor and allows a seasonal comparison based on different weather data and load profiles. Both the operating limits and the control range of the compressor are taken into account.

The operating limit of a chiller is defined by the most restrictive component. For compressors with a large operating range, it is therefore possible that the operating range is reduced by other components (e.g. expansion valve). This was not considered in this study and can be improved in further investigations.

Especially for large refrigeration capacities, several compressors are often operated in parallel. This increases the operational reliability due to redundancies and increases the control range of the refrigeration machine. In a next step, the evaluation method should be extended so that circuits with several compressors can also be evaluated.

The results show that in particular the desired refrigerant as well as the required refrigerating capacity strongly limit the available compressor types. The tool developed in this work checks which compressor designs are available for a given refrigeration capacity and refrigerant. Subsequently, the available compressor types are compared based on the defined location and load profile according to the method defined in this paper. The result is a ranking of the available compressor types according to aCOP.

The results of the tool were reviewed by the experts. To identify errors in the data acquisition (compressor polynomials) or evaluation method (aCOP), additional checks (e.g. by manufacturers) are useful.

Acknowledgements

The Authors would like to thank the Swiss Federal Office of Energy for their financial support in this project. In particular Mr. Martin Stettler is expressly thanked. Thanks for the valuable support and constructive cooperation also go to the contributing experts Claudio Müller, Jonas Schönenberger, Matthias Brügger, Rolf Löhner, Robert Dumortier, Michael Kriegers and Thomas Lang.

Nomenclature and Abbreviations

$aCOP$	Annual coefficient of Performance	T_{amb}	Ambient temperature
T_0	Evaporating temperature	ΔT	Temperature difference
T_c	Condensing temperature	SEER	Seasonal Energy Efficiency Ratio

References

- [1] EN 12900:2013 Refrigerant compressors - Rating conditions, tolerances and presentation of manufacturer's performance data, European Committee for Standardization CEN, Brussels BE.
- [2] EN 14825:2019 Air conditioners, liquid chilling packages and heat pumps, with electrically driven compressors, for space heating and cooling - Testing and rating at part load conditions and calculation of seasonal performance. European Committee for Standardization CEN, Brussels BE.
- [3] C. Stahel, L. Wick, and F. Tillenkamp, "Kälteverdichter – Schlüssel zur Energieeffizienz und Betriebssicherheit" IEF Energy Paper, Feb. 2022.
- [4] Energie Schweiz. Verdichter-Tool BFE www.bfe.admin.ch
- [5] H. Desmidt, K. Ekici and K. Young, „Computationally Efficient Axial Compressor Characteristic Map Generation Based on 1-D Meanline Approximation,“ Knoxville, Tennessee, 12.07.2013.